# Analysis of Calcium Deposits in Calcific Periarthritis

JUN'ICHIRO HAMADA, WATARU ONO, KAZUYA TAMAI, KOICHI SAOTOME, and TAKASHI HOSHINO

*ABSTRACT*. ***Objective.*** To determine if hydroxyapatite (HAP), octacalcuim phosphate (OCP), or tricalcium phosphate (TCP) can be found in the calcium deposits in calcific periarthritis.

***Methods.*** Thirty-six specimens from 34 patients who had acute inflammation and roentgenographically recognized calcification in soft tissue were analyzed. Twenty-three patients with calcific tendinitis in the shoulder and 11 with calcific periarthritis at other sites were included. We prepared 2 kinds of samples from each specimen; a dried sample (washed and dried calcific deposit), and a sample heated to 1000˚C. All were analyzed by X-ray diffraction, Raman spectroscopy, infrared absorption spectroscopy, and X-ray fluorescence spectrometry for calcium and phosphorus molar ratio. Synthetic HAP was used as the control in each analysis.

***Results.*** The X-ray diffraction patterns of all dried samples were similar to those of HAP and carbonate apatite. We found no diffraction patterns of OCP or TCP. However, an OH- group at 3570cm$^{-1}$ was observed with Raman spectroscopy for samples heated to 1000˚C and synthetic HAP, but not for the dried samples. Infrared absorption spectroscopy also confirmed an OH- group for samples heated to 1000˚C and synthetic HAP, and confirmed that dried samples contained carbonate.

***Conclusion.*** Calcium deposits are composed of carbonate apatite. HAP, OCP, and TCP were not identified in any deposits. (J Rheumatol 2001;28:809-13)

*Key Indexing Terms:*
BASIC CALCIUM PHOSPHATE
CALCIFIC PERIARTHRITIS
CARBONATE APATITE
HYDROXYAPATITE

The pathogenesis and dynamics of calcific periarthritis remains unclear 90 years after its presence was acknowledged by roentgenograms[1]. There is still no explanation for its diverse clinical course, phase of crystal formation, enlargement, disruption, or disappearance of calcium deposit. The first step in solving these issues should be to accurately determine the components of the calcific deposits. In previous studies, the deposits were shown to be composed of hydroxyapatite (HAP) utilizing X-ray diffraction (XRD) and infrared absorption spectroscopy[2-5]. Other studies demonstrated that the deposits were composed of carbonated apatite[6], octacalcium phosphate (OCP)[7], ß-tricalcium phosphate (TCP)[7], or calcium apatite with $CO_3^{2-}$ or $HPO_4^{2-}$ ion instead of the $PO_4^{3-}$ ion[8]. These different calcium phosphate crystals are grouped as basic calcium phosphate crystals[9]. However, it is difficult to differentiate HAP from calcium salts that possess similar diffraction characteristics by means of X-ray diffraction alone and to confirm the existence of an OH- group by infrared absorption spectroscopy. Therefore, the question remains whether calcific periarthritis is caused by HAP deposition.

We employed XRD, Fourier transform infrared spectroscopy (FTIR), Raman spectroscopy and X-ray fluorescence spectrometry (XRF) to analyze the calcific deposits from patients with calcific periarthritis to define the deposits in this disease.

*From the Department of Orthopaedic Surgery, Dokkyo University School of Medicine, Shimotuga, Tochigi, Japan.*

*J. Hamada, MD, PhD, Assistant Professor; W. Ono, MD, PhD, Assistant; K. Tamai, MD, PhD, Associate Professor; K. Saotome, MD, PhD, Professor; T. Hishino, MD, PhD, Professor Emeritus.*

*Address reprint requests to Dr. J.Hamada, 880 Kitakobayashi Mibumachi, Shimotuga, Tochigi, 321-0293, Japan.*

*Submitted October 19, 1999 revision accepted October 3, 2000.*

## MATERIALS AND METHODS

*Patients*. We collected 36 specimens from 34 patients who had acute inflammation and roentgenographically recognized calcification in soft tissue around the painful joint. Patients with calcium pyrophosphate dihydrate crystal deposition disease, collagen disease, chronic renal failure, or metabolic disorders were excluded from this study. Ages ranged from 22 to 71 years (average 54 years), and there were 8 males and 26 females. Twenty-three patients with calcific tendinitis or bursitis in the shoulder and 11 with calcific periarthritis (6 in the hand, 3 in the knee, 1 in the hip and 1 in the wrist) were included. All patients experienced sudden onset of moderate or severe pain around the joints without trauma and visited our clinic within one week of the onset of symptoms. Nine patients (26%) noted swelling and redness of the skin and all tenderness was confined to the affected joint. Roentgenographic examination revealed calcifications in soft tissue around the joints in all patients. Laboratory investigations revealed that C-reactive protein, white cell count, and erythrocyte sedimentation rate in peripheral blood were elevated in 30 patients (88%). Twenty-six specimens were aspirated by syringe, and 10 were removed surgically. The 26 fluid specimens aspirated contained many polymorphonuclear leukocytes on light microscopic examination. All patients took nonsteroidal anti-inflammatory drugs, and 22 were injected with corticosteroid at sites of calcification. Acute inflammation subsided by the 8th day of treatment on average ( range 2-29 days).

*Preparation of calcific deposits*. We prepared 2 kinds of samples from each specimen: dried samples were washed with distilled water and dried at room temperature; heated samples which were heated to 1000˚C for 1 hour. Synthetic HAP was provided by Sumitomo Cement Ltd. (Tokyo, Japan) as a control. All samples were analyzed by XRD,FTIR, Raman spectroscopy, and XRF spectrometry.

*XRD*. The powder X-ray diffraction patterns of all samples were recorded with a diffractometer (Ru-200B, Rigakudenki, Akishima, Japan) operated at a

scanning speed of 2˚2 θ/min using $CuK_\alpha$ (λ=0.154 nm) radiation generated at 30kV and 30mA from a graphite monochrometer. The detector was scanned between 3˚ and 90˚. A data processor ( RAD-B, Rigakudenki) was used to record radiation counts. The component of the specimens was defined according to the database of the Joint Committee on Powder Diffraction Standards (JCPDS).

*Raman spectroscopy*. Laser Raman spectra were collected from the powdered samples, which were loaded into the sample cups with a spectrometer (Ramanor U-1000, Jobin Yvon Ltd., Cedex, France) using excitation at 5145Å-ray of argon-ion laser with a NEC GLG3300 exciter. Scattered radiation was collected at 90˚ to the incident beam and detected by photon counting using a thermoelectrically cooled RCA C31034 photomultiplier tube. Laser power determined at the sample ranged from 100 to 150 mW. The spectrum scan speed was 120 $cm^{-1}$/min and repeated 30 times. Spectral ranges used were from 1800 to 120 $cm^{-1}$ and from 3700 to 3400 $cm^{-1}$.

*FTIR*. We obtained FTIR spectra between 4000 and 480 $cm^{-1}$ using a spectrometer (FTS-60, Bio-Rad Ltd, Massachusetts, USA) in conjunction with a microscope (IR-PLAN, Spectra Tech, USA). We placed the collected specimens on KRS-5 plates under stereomicroscope and performed direct measurements without using dispersion material such as KBr. Dry, $CO_2$-free nitrogen was used for purging of the spectrometer and the microscope. Spectra were obtained at 8 $cm^{-1}$ resolution and averaging 256 scans. We estimated carbonate content of the dried samples by the method of Featherstone[10].

*X-ray fluorescence spectrometry*. XRF was conducted using an X-ray analytical microscope (XGT-2000V, Horiba, Ltd., Kyoto, Japan). This apparatus analyzing each specimen in air without pre-treatment is able to calculate the Ca:P molar ratio. The measurement conditions consisted of an acceleration voltage of 15.0 kV, an irradiation current of 1.0 mA, an analyzing beam diameter of 100 $\mu$M, and a measurement time of 600 s. Synthetic HAP (Ca:P molar ratio of 1.67) and synthetic calcium pyrophosphate dihydrate (Ca:P molar ratio of 1.00) were used as controls. The characteristic intensities of calcium and phosphorus were measured at 3 spots on each dried sample and on each heated sample.

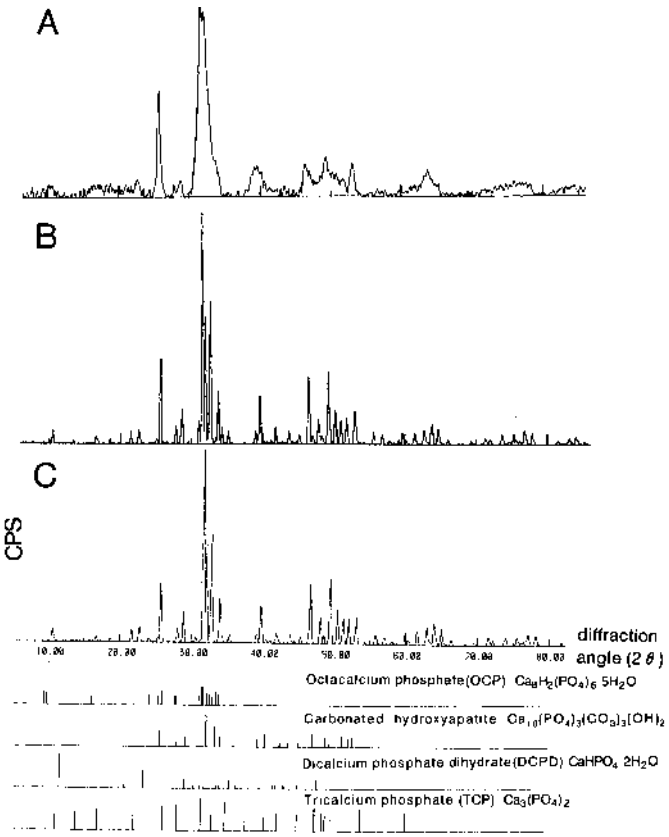


*Figure 1*. X-ray diffraction patterns of dried sample (A), heated sample to 1000˚C (B) and synthetic hydroxyapatite (C). X-ray diffraction spectra of octacalcium phosphate, carbonated hydroxyapatite, dicalcium phosphate, and tricalcium phosphate from JCPDS card are shown in the bottom.

## RESULTS

*XRD*. Figure 1 compares the powder XRD patterns of the dried sample, the heated sample, and the synthetic HAP. The XRD patterns of the former 2 samples consisted of a single apatitic phase. The 3 intensive peaks appearing in the vicinity of 25.9˚, 31.8˚, and 32.9˚ of 2 θ in the dried samples were similar to those of HAP and carbonate apatite. Phases characteristics of OCP, ß-TCP, and DCPD were not evident. Closer examination of their patterns revealed that the 36 dried samples had broader peaks than the heated samples and the synthetic HAP. Using XRD alone, HAP, carbonate apatite and calcium phosphate hydrate could not be differentiated from one another.

*Raman spectroscopy*. Raman spectra of dried samples, heated samples and synthetic HAP are shown in Figure 2. The spectra of all samples were characterized by a strong band at 960 $cm^{-1}$ derived from the symmetric stretching mode ($v_1$) of the $PO_4$-group. Other Raman-active phosphate modes were seen at approximately 1075 ($v_3$), 590 ($v_4$), and 435 $cm^{-1}$($v_2$). The weak bands at 1447, 1580, and 1650 $cm^{-1}$ were due to vibration modes of protein, specifically the $CH_2$ deformation, C=C symmetrical stretching mode, and amide band[11].

Since water is a weak Raman scatterer, adsorbed water, which can sometimes obscure parts of the infrared spectrum of calcium phosphate minerals, minimally affects the Raman spectrum[11]. The band positioned at 3570 $cm^{-1}$ attributed to the OH-group was clearly observed in the heated samples and the synthetic HAP. In contrast, the same band was absent in the dried samples. This indicated that the dried samples did not have the OH-group, and therefore did not contain HAP.

*FTIR*. Figure 3 shows the infrared spectra of the same samples used for XRD and Raman spectroscopy. The hydroxyl band at 3570 $cm^{-1}$ was evident in the heated samples and the synthetic HAP but unclear in the dried samples, because the broad water band from 3100 to 3700 $cm^{-1}$ covered the 3570 $cm^{-1}$ region.

Broad doublet-like bands in the range of 1600~1400 $cm^{-1}$ and at 870 $cm^{-1}$ characteristic of carbonate ions were clearly observed in the dried samples. However, these carbonate bands were present in neither the heated sample nor the synthetic HAP[12]. Figure 4 and Table 1 show the positions and prevalence of each carbonate band. We detected the band at 873 $cm^{-1}$ in all 36 dried samples (100%); the band at 1412 $cm^{-1}$ in 27 (75%); the band at 1450 $cm^{-1}$ in 36 (100%); the band at 1465 $cm^{-1}$ in 25 (69%); and the band at 1545 $cm^{-1}$ in 17 (48%). The estimated average carbonate content, calculated from spectra recorded in the linear absorption mode, was 8.6% for the dried samples.

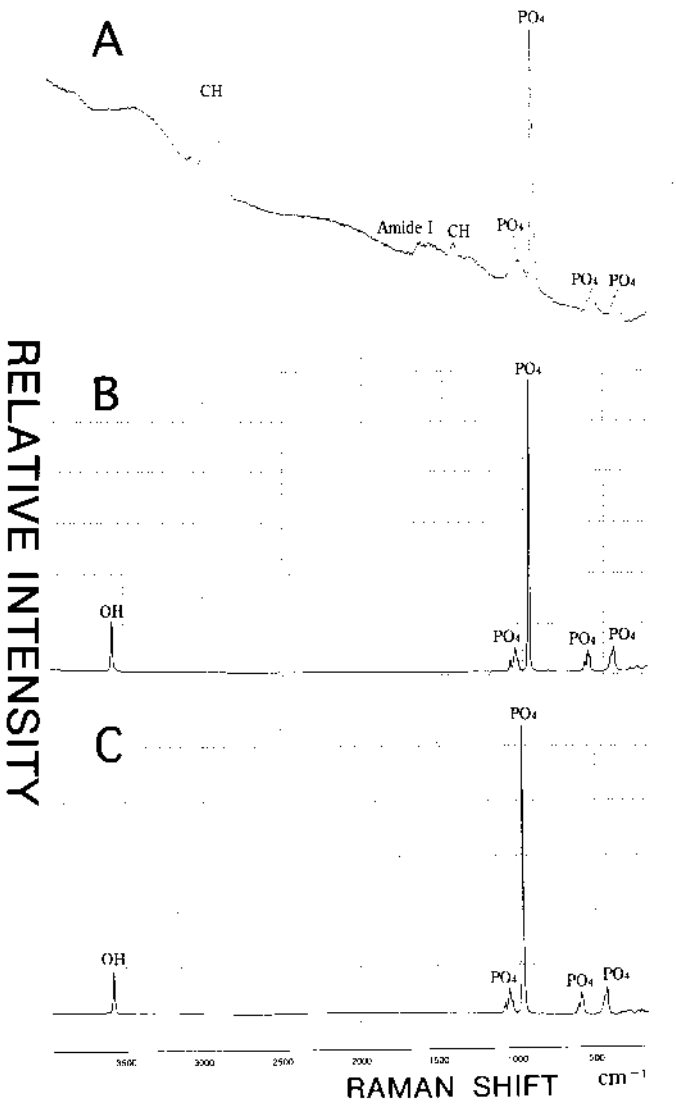


*Figure 2*. Raman spectra of dried sample (A), heated sample to 1000˚C (B) and synthetic hydroxyapatite (C).

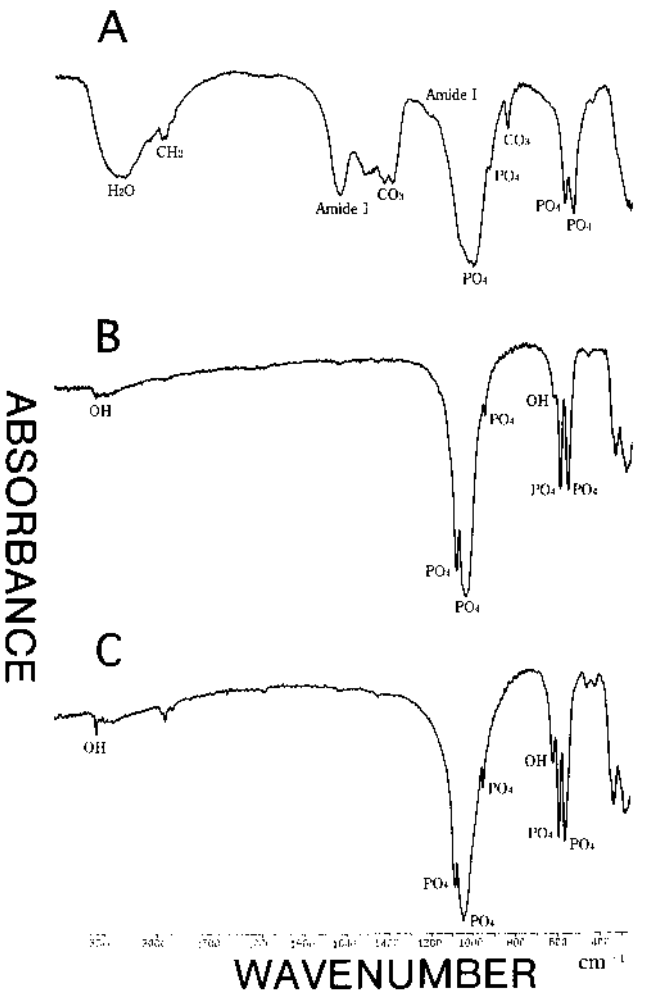


*Figure 3*. FTIR spectra of dried sample (A), heated sample to 1000˚C (B) and synthetic hydroxyapatite (C).

The bands at 1230, 1650, and 2920 $cm^{-1}$ in the dried samples were attributed to proteins bound to the dried samples, i.e., amideIII, amideI, and $CH_3$. Once dried samples were treated with hydrazine for deproteination, the intensity of each protein band became much weaker, although the intensities of carbonate bands did not change (data not shown). This indicated that protein still adhered to the dried samples, and that hydroxyl or phosphate ions had been replaced by carbonate in the calcium phosphate structure.

*Table 1*. Prevalence and infrared wavenumbers of carbonate bands in the dried samples.

| Wavenumbers ($cm^{-1}$) | 873 | 1412 | 1450 | 1465 | 1545 |
|---|---|---|---|---|---|
| Replaced ion Number/36 (%) | $PO_4$ 36 (100) | $PO_4$ 27 (75) | OH 36 (100) | $PO_4$ 25 (69) | OH 17 (47) |

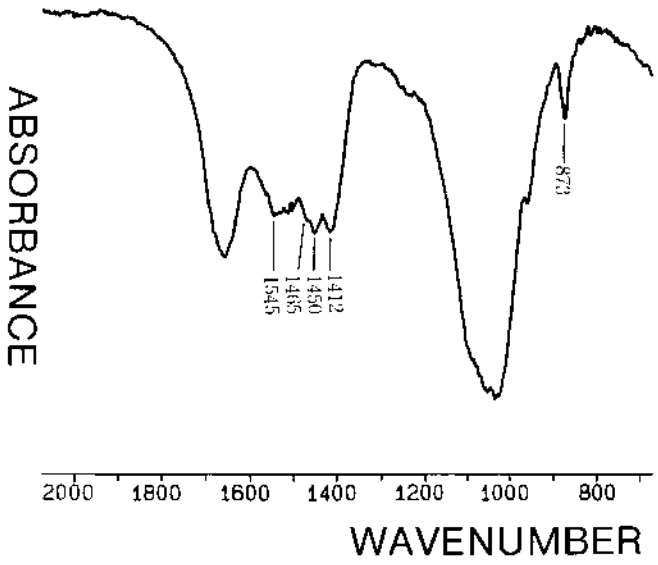


*Figure 4*. FTIR spectra of carbonate $v_2$,$v_3$ bands in dried sample.

*XRF*. Energy dispersive spectra of the dried samples revealed the presence of Ca and P. Bands of other ions such as Na and K were not obtained. Thirty-six dried samples had a Ca:P molar ratio of 1.85 ± 0.23, while the heated samples had ratio of 1.67 ± 0.02.

## DISCUSSION

XRD is a method of analysis used to characterize and identify crystals based upon their powder diffraction patterns. As Figure 1 shows, the XRD pattern of heated samples was exactly the same as that of the synthetic HAP, but slightly different from that of dried samples. The heated sample is composed of HAP, since its XRD pattern was clearly the same as that of synthetic HAP. The dried samples had broad peaks compared to those of the heated samples and the synthetic HAP. The broader peaks of the former are evidence that the dried samples have much lower crystallinity (crystal size, crystal imperfection, or both) than the heated samples and synthetic HAP[13] . This low crystallinity makes characterization of calcium deposits difficult. On the basis of JCPDS, the 3 strong peaks appearing in the vicinity of 25.8°, 31.7°, and 32.9° of 2 θ in the dried samples may have resulted from HAP, carbonate apatite, or calcium phosphate hydrate. Thus, XRD is unsuitable for use in differentiating these 3 substances. Our result is consistent with those of previous studies that these substances are indistinguishable with XRD alone[14-16].

If the dried samples are composed of calcium phosphate hydrate, this will be converted to ß-tricalcium phosphate by heating to 900°C[14]. However, the heated samples we examined were identified as HAP, indicating that the simply dried samples were composed of HAP or carbonate apatite, and not of calcium phosphate hydrate. Moreover, for all dried samples the hydroxyl band at 3570 $cm^{-1}$ was not present in Raman spectra (Figure 2). This shows that the dried samples do not possess an OH- group, and therefore do not consist of HAP. The major component of the dried samples is probably carbonate apatite.

The FTIR spectra of the heated samples and synthetic HAP were completely identifical (Figure 3). In addition, the infrared spectra of the dried samples had bands of a $PO_4$ group, a $CO_3$ group, protein and water. The hydroxyl bands at 630 and 3570 $cm^{-1}$ were present in the heated samples and the synthetic HAP, whereas the band at 630 $cm^{-1}$ was absent in the dried samples and the band at 3570 $cm^{-1}$ was not identifiable due to the broad band of absorbed water.

Theoretically, carbonate ions have 4 vibrational modes, 3 of which ($v_2$, $v_3$, and $v_4$) are observed in the FTIR spectrum[12]. The $v_4$ $CO_3$ domain has very low intensity bands and is seldom observed in the infrared spectrum[17]. Carbonate ions can be incorporated into the $PO_4$ and OH sites of the apatite lattice, giving rise to the B-type and A-type substitutions, respectively[18,19]. Based on polarized absorption spectra, Elliot[19] demonstrated that 2 substitutions of carbonate gives rise to distinct absorption bands at 1465 ($v_3$), 1412 ($v_3$), and 873 ($v_2$) $cm^{-1}$ for B-type ($PO_4$ site) and at 1545 ($v_3$), 1450 ($v_3$), and 879 ($v_2$) $cm^{-1}$ for A-type (OH site). The findings that the prevalence of the band at 1450 $cm^{-1}$ is 100% and that the hydroxyl band at 3570 $cm^{-1}$ is absent in Raman spectra of the dried samples indicate complete occupation of OH sites by carbonate. Prevalence of the hydroxyl band at 1545 $cm^{-1}$ was the lowest among carbonate bands. The carbonate band at 1545 $cm^{-1}$, associated with the replacement of hydroxyl ions, is due to surface-adsorbed carbonate and is thermodynamically less stable than the other carbonate sites[12]. On the other hand, phosphate bands were observed in both Raman and FTIR spectra of all dried samples, indicating that substitution of carbonate for $PO_4$ sites was incomplete.

The dried samples had large Ca:P molar ratios (1.85 ± 0.23), because most of their $PO_4$ sites, if not all, were replaced by carbonate. Our result is consistent with that of a previous study that found a positive correlation between Ca:P molar ratio and percent carbonate[12]. The Ca:P molar ratio is known to differ among calcium phosphate crystals. However, it cannot be used as an indicator of the presence of a specific calcium phosphate crystal, since the Ca:P molar ratio varies depending on the biological conditions in which a calcium phosphate crystal is produced. The carbonate apatite in calcific periarthritis is indicated by the formula:

$$Ca_{10-x-y/2}(PO_4)_{6-x}(CO_3)_x(OH)_{2-y}(CO_3)_{y/2} \cdot nH_2O$$
$$(0 < x > 4,\ y = 2)$$

The finding that calcium deposits in calcified periarthritis are composed of carbonate apatite may enable new understanding of crystal formation, inflammatory reaction and absorption of crystals. The mechanism of calcium deposition in calcific periarthritis is still unclear. Only a few *in vitro* models have been published for study of apatite mineralization, including those for kidney stones[20] and an osteoblastic cell culture[21]. Generally, the apatite formation requires elevated Pi and $Ca^{2+}$ levels, and alkaline phosphatase (ALPase) activity[22]. The gel and other inorganic crystallization models usually used were saturated or supersaturated solutions of Pi and $Ca^{2+}$ with or without macromolecular components for crystallization[23]. Crystallization of apatite in soft tissue does not readily occur without matrix vesicles or elevation of ALPase activity under the conditions present in human extracellular fluid: [$Ca^{2+}$] 1~2 mM, [Pi] 1 mM, temperature 37°C, pH 7.4. Nanobacteria, which are the smallest cell-walled bacteria recently discovered to be present in human and bovine blood, produce carbonate apatite[24]. This apatite was formed at [$Ca^{2+}$] 1.8 mM and [Pi] 0.9 mM or less, without replenishment of the medium, in a nanobacteria model[24]. Nanobacteria can form carbonate apatite under physiological conditions. We speculate that nanobacteria may play a role in forming calcium deposits in calcific periarthritis. Immunohistochemical study and detection of bacteria in serum of patients with calcific periarthritis will be required to

determine the relationship between nanobacteria and BCP crystal deposition disease.

The inflammatory potential of BCP crystals has been studied. Prudhommeaux, *et al*, using the rat air pouch, reported that the inflammatory potential of BCP crystals appeared to vary according to 2 crystal features, specific surface area and the Ca:P ratio[25]. In their study, 2 kinds of B-type carbonate apatites (3.2 and 6.9% of carbonate), stoichiometric HAP, and nonstoichiometric HAP incorporating carbonate were prepared. Maximum white blood cell counts exceeded 60,000/mm$^3$ with 2 kinds of carbonate apatites and nonstoichiometric HAP, but were less than 30,000/mm$^3$ with stoichiometric HAP. These carbonate apatites had 1.34 and 1.30 in Ca:P molar ratio, which were so different from 1.85 in our dried samples. The discrepancy is caused by the fact that 1.34 and 1.30 were the Ca/(P+$CO_3$) molar ratio, whereas 1.85 was a Ca:P molar ratio. Increase in carbonate concentration makes apatite crystals less in a Ca:(P+$CO_3$) ratio, more in a Ca:P ratio, smaller in size and wider in specific surface area, indicating significant inflammatory potential[26]. HAP has been used in orthopaedic practice, as a bone filler as well as for artificial bones and joints. However, inflammatory reactions have not been observed around the implanted HAP, except for some giant cells[27]. In addition, carbonate apatite has been provided as an injectable material of paste-like consistency for the treatment of unstable fractures[28]. Carbonated apatite cement used for the treatment of distal fractures of the radius induces severe inflammation if it leaks into the soft tissue[29]. The severe inflammation often seen in calcific periarthritis may be due to carbonate apatite.

The calcium deposits visible on x-ray in which conditions may undergo spontaneous resorption after acute inflammation, indicates that crystal dissolution may be preceded by endocytosis from the periphery of the deposit. The solution composition for sintered carbonate apatite at 30 seconds is comparable to that of sintered HAP at 3.8 days with respect to degree of supersaturation[15]. The presence of carbonate provides greater specific surface area than obtained with HAP[13]. Since calcium deposits are composed of carbonate apatite, resorption of the calcium can usually be observed in the natural course of calcific periarthritis.

We conclude that calcium deposits in calcific periarthritis are composed of carbonate apatite. Our result may reasonably explain the clinical course of the disease, including the phase of crystal formation, enlargement, disruption, inflammation, and resorption.

## REFERENCES


1. Painter CF. Subdeltoid bursitis. Boston Med Surg J 1907;156:345-9.
2. Dieppe PA, Huskisson EC, Crocker P, et al. Apatite deposition disease. A new arthropathy. Lancet 1976;7:266-9.
3. Schumacher HP, Miller JL, Ludivico C, et al. Erosive arthritis associated with apatite crystal deposition. Arthritis Rheum 1981;24:31-7.
4. Boskey AL, Bullough PG, Vigorita V, et al. Calcium-acid phospholipid phosphate complexes in human hydroxyapatite-containing pathologic deposits. Am J Pathol 1988;133:22-9.
5. Gärtner J, Daculsi G. Analysis of calcific deposits in calcifying tendinitis. Clin Orthop 1990;254:111-20.
6. Faure G, Daculsi G, Netter P, et al. Apatites in heterotopic calcifications. Scan Microsc 1982;4:1629-34.
7. McCarty DJ, Lehr JR, Halverson PB. Crystal population in human synovial fluid. Identification of apatite, octacalcium phosphate and tricalcium phosphate. Arthritis Rheum 1983;26:247-51.
8. Saez-Clavere L, Legros R, Bonel AG. Étude cristallochimique de deux calcifications sous-deltoïennes. Revue du Rheum 1980;47:383-92.
9. Halverson PB, McCarty DJ. Basic calcium phosphate (Apatite, octacalcium phosphate, tricalcium phosphate) crystal deposition diseases. In: Koopman BC, editor. Arthritis and allied condition. Philadelphia:Lea & Febiger;1996:2127-46.
10. Featherstone JDB, Peason S, LeGeros RZ. An infrared method for quantification of carbonate in carbonated apatites. Caries Res 1984;18:63-6.
11. Sauer GR, Zunic WB, Durig JR, et al. Fourier transform Raman spectroscopy of synthetic and biological calcium phosphates. Calcif Tissue Int 1994;54:414-20.
12. Nelson DG, Featherstone JDB. Preparation, analysis, and characterization of carbonated apatites. Calcif Tissue Int 1982; 34:S69-S81.
13. Doi Y, Moriwaki T, Aoba T, et al. ESR and IR studies of carbonate-containing hydroxyapatites. Calcif Tissue Int 1982;34:178-81.
14. Posner AS, Stephenson AS. Crystallographic investigation of tricalcium phosphate hydrate. J D Res 1952;31:371-82.
15. Doi Y, Shibatani Y, Kajimoto T, et al. Sintered carbonate apatite as bioresobable bone substitutes. J Biomet Mater Res 1998;39:603-10.
16. Rehman I, Knowels JC, Bonfield W. Analysis of in vitro reaction layer formed on bioglass using thin-film X-ray diffraction and ATR-FTIR microspectro-scopy. J Biomed Mater Res 1998;41:162-6.
17. Feki HE, Rey C, Vignoles M. Carbonate ions in apatites: Infrared investigation in the v4 $CO_3$ domain. Calcif Tissue Int 1991;49:269-74.
18. Elliot JC, Holcomb DW, Young RA. Infrared determination of the substitution of hydroxyl by carbonate ions in human dental enamel. Calcif Tissue Int 1985;37:372-5.
19. Legeros RZ, Trautz OR, Klein E, et al. Two types of carbonate substitution in the apatite structure. Experientia 1969;24:5-7.
20. McLean R, Nickel JC, Beveridge TJ, et al. Observations of the ultrastructure of infected kidney stones. J Med Microbiol 1989;29:1-7.
21. Stanford CM, Jacobson PA, Eanes ED, et al. Rapidly forming apatitic mineral on an osteoblastic cell line (UMR-01 BSP). J Biol Chem 1995;270:9420-8.
22. Anderson HC. Mechanism of pathological calcification. Crystalline deposition diseases. Rheum Dis Clin North Am 1988;14: 303-19.
23. Cheng P. Pathologic calcium phosphate deposition in model system. Crystalline deposition diseases. Rheum Dis Clin North Am 1988;14:341-51.
24. Kajander EO, Çiftçioglu AN. Nanobacteria: An alternative mechanism for pathogenic intra- and extracellular calcification and stone formation. Pro Natl Acad Sci 1998;95:8274-79.
25. Prudhommeaux F, Schiltz C, Lioté F, et al. Variation in the inflammatory properties of basic calcium phosphate crystals according to crystal type. Arthritis Rheum 1994;39:1319-26.
26. Shimoda S, Aoba T, Moreno EC, et al. Effect of solution composition on morphological and structural features of carbonate apatites. J Dens Res 1990;69:1731-40.
27. Hoogendoorn HA, Renooij W, Akkermans LMA et al. Long-term study of large ceramic implants (porous hydroxyapatite) in dog femora. Clin Orthop 1984;187:281-8.
28. Constantz BR, Ison IC, Fulmer MT, et al. Skeletal repair by in situ formation of the mineral phase of bone. Science 1995;267:1796-9.
29. Kopylov P, Jonsson K, Thorngren KG, et al. Injectable calcium phosphate in the treatment of distal radial fracture. J Hand Surg 1996;21B:768-71.